

# AN IDENTIFICATION OF G.654-FIBERS BASED ON ANALYSIS OF THE MANDELSTAM – BRILLOUIN SCATTERING CHARACTERISTICS IN OPTICAL FIBERS

DOI: 10.36724/2072-8735-2025-19-12-51-58

Manuscript received 07 September 2025;

Accepted 24 November 2025

**Igor V. Bogachkov,**  
Omsk State Technical University (OmSTU), Omsk, Russia,  
[bogachkov@mail.ru](mailto:bogachkov@mail.ru)

**Keywords:** single-mode optical fiber, Mandelstam - Brillouin scattering, Brillouin reflectogram, Brillouin backscattering frequency profile, G.654-optical fiber, detection of the optical information leakage channel, information security of the fiber-optic telecommunication system

In today's rapidly changing world, the range of manufacturers of various optical materials, which are currently used in the production of optical fibers (OFs), and later optical cables, has significantly expanded in the Russian Federation. Identifying the different types of single-mode optical fibers in previously laid and currently being laid cables and determining their characteristics is a pressing issue. Based on the identified Mandelstam – Brillouin scattering parameters, it is possible to identify sections of the light wave-guides that have differences in the strain parameters. This is the basis of the Brillouin reflectometry method, which is used for early detection of potentially unreliable sections in fiber light wave-guides. At the same time, a particularly important problem is to identify specific types of fibers from different manufacturers that have the same type and common purpose. The data of experimental testing of the frequency parameters of the Mandelstam – Brillouin back scatter in light wave-guides which were contained from different sections of various fiber kinds (with various temperature factors and longitudinal strain) using the Brillouin optical time-domain reflectometer (BOTDR) are analyzed in this work. The special attention was paid to the types of the G.654-fibers (G.654 is a recommendation by ITU-T which determine parameters of single-mode shifted cut-off wavelength fibers), which was developed for high-speed long-distance optical telecommunication systems. Based on experimental researches using BOTDR reflectograms, the values of Brillouin frequency shift (BFS) under normal conditions were calculated for all tested types of G.654 type fibers, and their frequency parameters were determined. The obtained in experimental researches of Brillouin reflectograms (including temperature changes) are presented. Frequency characteristics for each tested type of optical fibers are given in this work. Combining the tested sections of various types of single-mode OF into a common light guide significantly reduces the time to remove frequency and other characteristics of the spectrum. BOTDR reflectograms for the entire light guide are determined simultaneously, and then the frequency parameters (including the spectrum characteristics) for each section are analyzed. The differences between graphs of different fiber types are clearly visible. The differences in the frequency characteristics of the Brillouin backscatter and the values of the BFS can be used to automate the processing of BOTDR reflectograms and the classification of varieties of OFs.

#### Information about author:

**Igor V. Bogachkov,** Professor of "Communication means and information security" department of the Omsk State Technical University (OmSTU), Adv. Dr., Docent, Senior Member IEEE, Omsk, Russia, [bogachkov@mail.ru](mailto:bogachkov@mail.ru). ORCID ID 0000-0002-7019-1784

#### Для цитирования:

Богачков И.В. Выявление разновидностей одномодовых оптических волокон со смещённой длиной волны отсечки на основе анализа характеристик рассеяния Манделштама – Бриллюэна // Т-Комм: Телекоммуникации и транспорт. 2025. Том 19. №12. С. 51-58.

#### For citation:

Igor V. Bogachkov, "An Identification of G.654-Fibers Based on Analysis of the Mandelstam – Brillouin Scattering Characteristics in Optical Fibers," *T-Comm*, 2025, vol. 19, no. 12, pp. 51-58.

In today's rapidly changing world, the list of producers of the optical substances (such as “blanks”, “preforms”), using in the manufacturing of optical fibers considerably is expanded in Russia.

Identifying the various kinds of optical fibers in laid and currently being laid cables and detecting their characteristics is the pressing issue [1-6].

Mandelstam – Brillouin scattering is the fundamental nonlinear optical phenomenon which appears when light interacts with acoustic waves in a material environment. Based on the identified Mandelstam – Brillouin back-scattering (MBB) parameters (such as the changes in the power level of the back-reflected signal, the frequency graphs of Mandelstam – Brillouin back scatter, the Brillouin frequency shift (BFS), etc.) it is possible to identify sections of the light wave-guides that have differences in the strain parameters of optical fibers [6-15]. This is the basis of the Brillouin reflectometry method, which is used for early detection of potentially unreliable sections in fiber light wave-guides [3-6]. The frequency of the main maximum (“peak”) of the MBB spectrum characteristic is determined as the Brillouin frequency shift (BFS).

The linear dependence of BFS on temperature influence is used in distributed temperature sensors. And linear dependence of BFS on longitudinal tension is used in strain sensors for monitoring bridges (pipelines, etc.) and for monitoring of physical state of optical fibers. The power of the Brillouin back-scatter light-wave signal depends on the electrostriction coefficient of the material and the acoustic-optical interaction.

It should also be noted that some methods of forming information leakage channels from optical fiber, based on temperature, mechanical and acoustic actions on the fiber, can be detected using the analysis of Brillouin backscatter parameters [5, 6].

The methods for determining BFS are as follows: a coherent detection, a time-domain correlation analysis, and a heterodyne detection. A coherent detection method that provide a sub-centimeter spatial resolution, which is critical for monitoring microstructural changes. A time-domain correlation analysis, which allows high-resolution measurements up to 100 km. A heterodyne detection is used for accurate BFS measurement with a high spatial resolution of up to 0.1 MHz. This method is based on mixing probing and Stokes propagated light signals with subsequent spectral signal analysis, and is used in the Brillouin optical time-domain reflectometer (BOTDR) [3-6], which experimental results for various kinds of optical fibers (OFs) are analyzed in this work.

At the same time, a particularly important problem is to identify specific types of fibers from different manufacturers that have the same type and common purpose.

The physical properties of the optical fiber core material play a crucial role for resulting spectrum parameters of the Mandelstam – Brillouin scattering. Doping the optical fiber core with various alloying additives we can a significant change of the parameters of the speed of hyper-acoustic waves, MBB frequency characteristics and Brillouin frequency shift.

The experimental research data of the frequency parameters of the Mandelstam – Brillouin back scatter in light wave-guides which were contained from different sections of various fiber kinds (with various temperature factors and longitudinal strain) using the Brillouin optical time-domain reflectometer (BOTDR) are analyzed in this work.

The special attention was paid to the types of the G.654-fibers (G.654 is a recommendation by ITU-T which determine parameters of single-mode shifted cut-off wavelength fibers), which was developed for high-speed long-distance optical telecommunication systems. This type of fibers has low losses. The lower values of specific attenuation were obtained (up to 0.168 dB/km at the wavelength ( $\lambda$ ) of 1.55  $\mu\text{m}$ ) in later versions of G.654-fibers [4].

Since noticeable changes in the MBB characteristics can be detected in various kinds of the G.654-fibers, it is necessary to measure Brillouin reflectograms at various conditions and influences on G.654-fibers, etc.

The results of the author's earlier studies of OF-G.654 and other single-mode OF are presented in [3-6, 13, 14].

With the assistance of CJSC “Moskabel-Fujikura” (Moscow), using BOTDR “Ando AQ 8603” experimental researches were carried out for all testing types of fibers.

The type G.654-E of fibers with cut-off wavelength has been thoroughly tested. This fiber type is characterized by ultra-low attenuation, low macrobending losses, and a large effective area.

The G.654 fibers of various producers were made available for the experimental researches in collaboration with CJSC “Moskabel-Fujikura” company and the JSC “Optic Fiber Systems” company employees.

The light wave-guide was formed from normalizing coil (the first OF (the recommendation by ITU-T is G.652), which length is 1 km approximately) and the sections of the testing fiber varieties, which were connected in series.

The main experiments assume that the test material is at room temperature and is not subjected to any mechanical stress (the so-called – “normal conditions”).

The spatial distribution of the MBB spectrum (BOTDR 3D-reflectogram) for the light wave-guide, which was made up of OF-G.652 and OF-G.654-E-Sar (The fiber of the JSC “Optical Fiber Systems” – Saransk), is presented in Fig. 1. In the right lower corner, the MBB frequency characteristic and Brillouin frequency shift value ( $f_B$ ) of this (G.654-E-Sar) fiber in Fig. 1 are shown.

In all reflectograms presented below, in the lower left corners of the graphs, the lower frequency value of the scan range is presented as “Start” (in the case in Fig. 1, the initial frequency is 10.900 GHz), the finish (upper) frequency value of the scan range is indicated as “Stop” (in this example for Fig. 1, the frequency is 11.145 GHz), and the scan frequency step (“Sweep”) in this example for Fig. 1 is 5 MHz.

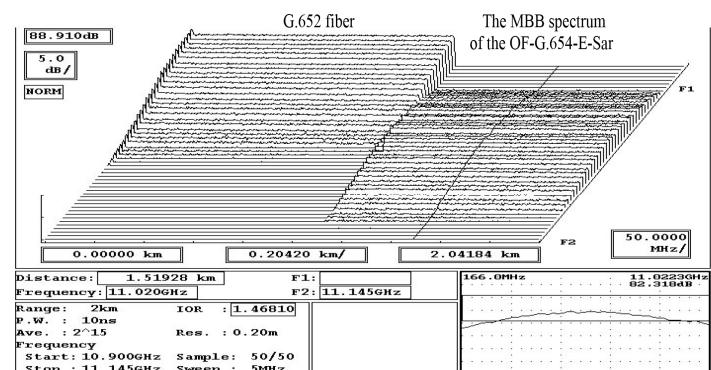


Fig. 1. The BOTDR 3D-reflectogram of the MBB frequency characteristic of the G.654-E-Sar fiber

The corresponding BOTDR-multireflectogram of the G.654-E-Sar fiber in Fig. 2 is presented.

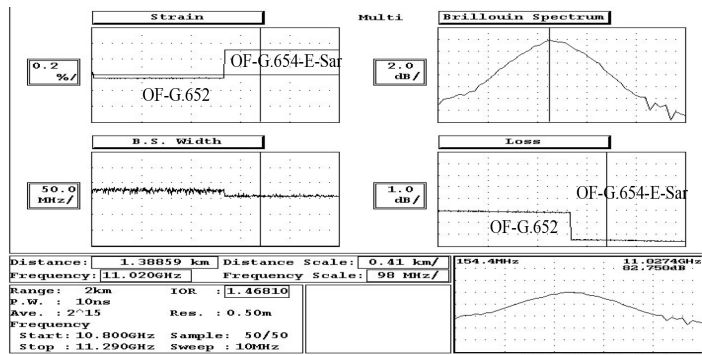


Fig. 2. The Brillouin multi-reflectogram of the of the G.654-E-Sar fiber

In Fig. 2 we can observe “Strain” – the dependence of tension on the length of the light wave-guide. “Brillouin Spectrum” in Fig. 2 is the MBB frequency characteristic, “B.S. Width” is the width of the MBB frequency characteristic, and “Loss” is the back-reflected MBB signal level along the light wave-guide.

Fig.3 shows a 3D BOTDR reflectogram (in the section of the light wave-guide after OF-G.652, the following varieties of G.654 fibers are connected together:

“Fujikura nature” (abbreviated designation is “FujN” – the attenuation coefficient at the wavelength of 1.55 μm was 0.167 dB/km),

“Corning ULL” fiber (abbreviated designation is as “Cor” – the attenuation coefficient at the wavelength of 1.55 μm was 0.187 dB/km), and fiber “Fujikura guide TM” (abbreviated as “OF-FujT” – “HTC-110” was the attenuation coefficient 0.167 dB/km at the wavelength of 1.55 μm, and the attenuation coefficient of “HTC-125” was 0.164 dB/km at the wavelength of 1.55 μm).

It should be noted that the “Strain” dependences in the BOTDR “Ando AQ 8603” is calculated by the formula:

$$\text{“Strain”} [\%] = (f_B [\text{GHz}] - f_0 [\text{GHz}]) / 0.493 [\text{GHz} / \%] \propto (f_B - f_0) / f_0, \quad (1)$$

where the reference frequency value ( $f_0$ ) is typically set (by default) for G.652 fiber under the normal conditions ( $f_0$  is 10.85 GHz), and coefficient “0.493 [GHz / %]” is determined by the light source’s wavelength of 1.55 microns.

Therefore, it is advisable to interpret this graph in this case as the relative change in BFS along the light wave-guide.

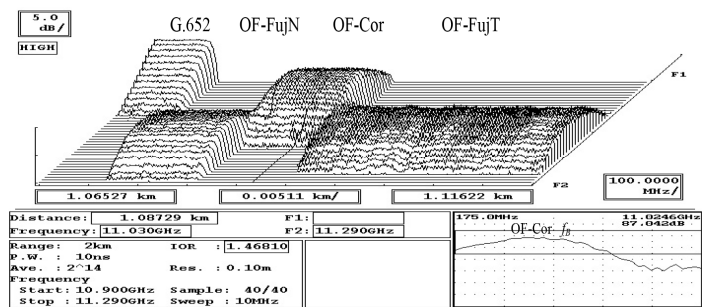


Fig. 3. The reflectogram of the MBB frequency characteristic of the light wave-guide with G.654 fiber sections of various kinds

Fig. 4 the corresponding multireflectogram indicating the characteristic areas is presented.

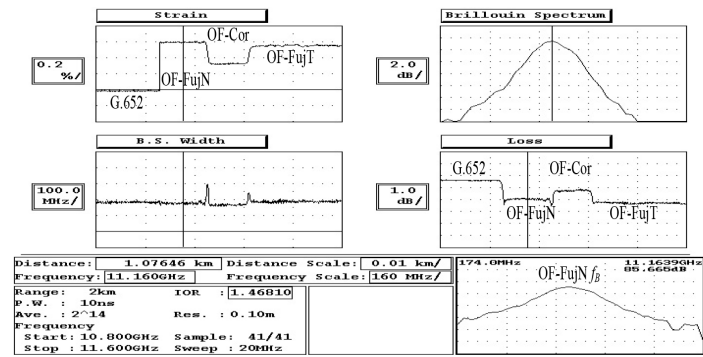


Fig. 4. Brillouin multireflectogram for the light wave-guide with G.654 of different types

The MBB frequency characteristic and Brillouin frequency shift value of the G.654-E-FujN fiber in the right lower corner of this figure are shown. The value of the BFS under normal conditions for OF-FujN was 11.16 GHz, for OF-Cor was 11.03 GHz, and for OF-FujT was 11.14 GHz. The differences in the characteristics of MBB frequency characteristic and BFS are clearly visible.

Characteristic “spikes” oftentimes are observed on multireflectograms in the of MBB spectral width dependencies (“B.S. Width”) along the light wave-guide length at the junctions of different fiber types (and also under varying temperatures along the single fiber section). This is mainly due to the fact that such locations (e.g., fiber splice points) have a length much smaller than the spatial resolution of BOTDR. Consequently, this leads to the “overlap” of the MBB spectrums in these locations, resulting in spectral broadening and, accordingly, a “spike” on the graphs. Changes in “Loss” graphs can also be observed when there are differences in the optical properties of the fibers being joined.

When splicing sections of the single fiber under identical conditions, such an effect is not observed on the spectral width (“B.S. Width”) graphs along the optical wave-guide. Only small “step-like” changes, related to the quality of the spliced joint, may be observed on the “Loss” graphs.

Figure 5 shows the 3D BOTDR reflectogram of the MBB frequency characteristic along the light wave-guide (G.652 is a normalizing coil; the remaining G.654 are: “Fujikura guide H” (G.654-E, abbreviated designation is “FujH” – the attenuation coefficient at the wavelength of 1.55 μm was 0.167 dB/km), “Fujikura Pure Advance 80” (G.654-C, abbreviated designation is “FujP80” – the attenuation coefficient at the wavelength of 1.55 μm was 0.166 dB/km), “Fujikura Pure Advance 110” (G.654-E, abbreviated designation is “FujP110” – the attenuation coefficient at the wavelength of 1.55 μm was 0.165 dB/km), and erbium doped optical fiber – (abbreviated designation is “ErDF”).

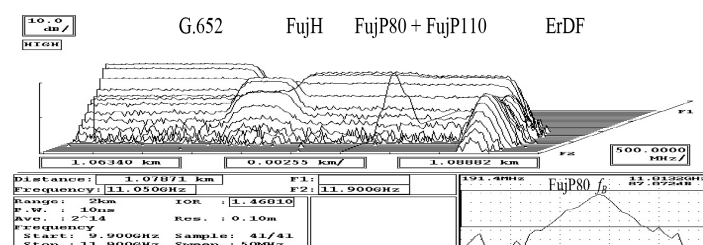


Fig. 5. The BOTDR 3D-reflectogram of the MBB frequency characteristic of the light wave-guide with G.654 sections of different types

The MBB frequency characteristic and Brillouin frequency shift value of the “FujP80” fiber in the right lower corner of this figure are shown. The corresponding Brillouin multireflectogram is presented in Fig. 6.

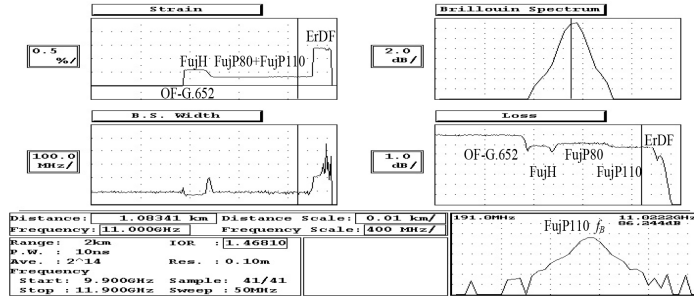


Fig. 6. Brillouin multireflectogram of the light wave-guide with G.654 sections of different types

The MBB frequency characteristic and Brillouin frequency shift value of the “FujP110” fiber in the right lower corner of this figure are shown. The value of the BFS under normal conditions for the “FujH” fiber was 11.17 GHz, for the “FujP80” fiber is 11.01 GHz, and for the “FujP110” fiber is 11.02 GHz.

ErDF was used as an “absorber” of the residual signal. The “outlier” on the graph of the level of the back-reflected signal of ErDF in the end of the light wave-guide is distinguished.

The sections of the light wave-guide containing locations with various fiber types have different MBB frequency characteristics and BFS values, allowing the researcher to distinguish between sections with different fiber types.

It is possible to set the initial value for each variety (under normal conditions) BFS ( $f_{B0}$ ) of G.654 fibers, according to the researched 3D-reflectograms of the MBB spectrum of the BOTDR.

The values of the “peaks” (“maximums” of the spectrum parameters) of the MBB frequency characteristics for all tested types of G.654 fibers recommendations from different manufacturers are shown in Table 1. Results of some other G.654 fiber kinds researched earlier [4, 5] are presented too.

Table 1 shows that all the researched fibers have the frequency shift greater than 11 GHz, and that different types of fibers have different in the MBB frequency characteristics and BFS values. For example, under normal conditions, the Brillouin frequency shift value of the conventional G.652 fiber (a cut-off wavelength is 1.26  $\mu\text{m}$ , as well as for fiber G.657) is approximately 10.4 GHz, for the G.652 fiber with a cutoff wavelength of 1.35  $\mu\text{m}$  (provided by the Saransk “Optical Fiber Systems”), it is 10.78 GHz, and the BFS of the G.652 fiber with a cutoff wavelength of 1.23  $\mu\text{m}$  (provided by the JSC “Optical Fiber Systems”) is 10.81 GHz.

Table 1

Types of G.654-fibers (a cut-off wavelength is at least 1.53 microns)	Average values of the $f_{B0}$ , GHz
G.654-E-FujH	11.17
G.654-E-FujN	11.16
G.654-E-FujT	11.15
G.654 Corning ULL	11.04
G.654-E-FujP110	11.03
G.654-C-FujP80	11.02
G.654-E-Sar	11.02

The differences between the fiber varieties in their MBB characteristics and BFS values are related to the difference in the structure of the core layers (albeit insignificant) in thickness, composition, and the degree of concentration of the substances used in them [3-14].

Experimental Brillouin reflectograms were also measured when heating the light wave-guide composed of the tested types of fibers (including G.654 fibers) to the temperature of +70°C.

Figure 7 shows the 3D BOTDR reflectogram of the MBB frequency characteristic along the light wave-guide (with heated sections) composed of the following fibers: G.652, “FujN”, “Cor”, and “ErDF”. Heated regions stand out on the graphs owing to substantial alterations in spectral characteristics. The displacement of the frequency characteristics of MBB (and respectively the BFS values) is observed in the positive direction of the frequency axis on the reflectograms.

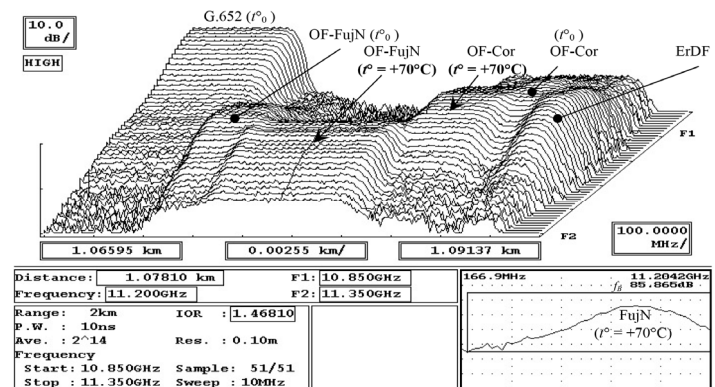


Fig. 7. The BOTDR 3D-reflectogram of the MBB frequency characteristic of the light wave-guide with heated sections of the “FujN” and “Cor” fibers

Figure 8 shows the 3D BOTDR reflectogram of the MBB frequency characteristic along the light wave-guide (with heated sections) composed of the following fibers: G.652, “FujN”, “FujP80”, “FujP110” and “ErDF”.

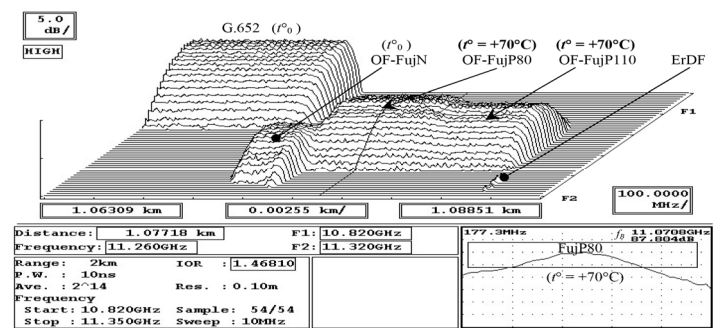


Fig. 8. The BOTDR 3D-reflectogram of the MBB frequency characteristic of the light wave-guide with heated sections of the “FujN”, “FujP80” and “FujP110” fibers

The corresponding Brillouin multireflectogram is presented in Fig. 9.

The “Strain” dependencies of the multireflectograms was observed an increase of the tension in heated sectors. At the same time, the “Loss” graphs of the multireflectograms clearly visible an increase in the level of the back-reflected MBB signal in heated sectors.

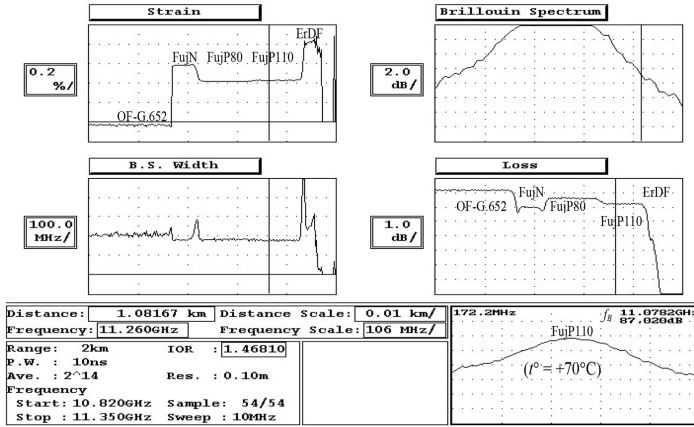


Fig. 9. The Brillouin multireflectogram of the light wave-guide with heated sections of the "FujN", "FujP80" and "FujP110" fibers

The dependence of the BFS displacement on temperature ( $t^\circ$ ) is described by the following formula:

$$t^\circ - t_0^\circ [^\circ\text{C}] = (f_B [GHz] - f_{B0} [GHz]) / 1.07 [GHz / ^\circ\text{C}] \propto (f_B - f_{B0}) / f_{B0}, \quad (2)$$

where  $t_0^\circ$  is the temperature of the unheated section,  $f_{B0} = f_B(t_0^\circ)$ .

The average value of the BFS displacements for all tested fibers was approximately 0.05 GHz. For the "FujN" fiber BFS was observed at the frequency of 11.20 GHz (at  $f_{B0} = 11.16$  GHz). For the fiber "Cor" it was 11.09 GHz ( $f_{B0}$  is 11.04 GHz), for the "FujP80" fiber it was 11.07 GHz (at  $f_{B0} = 11.02$  GHz), for the "FujP110" fiber it was 11.08 GHz ( $f_{B0}$  is 11.03 GHz).

The Brillouin frequency shift  $f_B$  in the optical fiber is the fundamental parameter in distributed sensing and telecommunication systems. It is determined by the acoustic-optical interaction between the incident light and thermally induced acoustic waves propagating along the fiber core. This interaction produces the frequency-shifted back signal (MBB), the characteristics of which depend on the optical and mechanical properties of the medium.  $F(r)$  is of the main optical mode amplitude distribution of the fiber [7].

The main light mode behavior  $L(r)$  is defined by next formula:

$$\frac{\partial^2 L(r)}{\partial r^2} + \frac{\partial L(r)}{r \partial r} + \left( n(r) \left( \frac{\omega_L}{c} \right)^2 - (\beta_L)^2 \right) L(r) = 0. \quad (3)$$

where  $\beta_L$  is the phase coefficient,  $\omega_L = 2\pi f_L = 2\pi c / \lambda_L$  ( $\lambda_L$  is the laser wavelength),  $n(r)$  is the refractive index as function of the fiber radius,  $c$  is the velocity of light.

In case of several fiber layers, the optical properties of which are different,  $F(r)$  should be found by formulas:

$$F(r) = \begin{cases} A_0 J_0(u_1 r) & , \text{if } r \leq a_1; \\ A_{j1} J_0(u_j r) + A_{j2} N_0(u_j r) & , \text{if } a_{j-1} < r \leq a_j; \\ A_N J_0(a_{N-1} u_j) K_0(wr) / K_0(a_{N-1} w) & , \text{if } a_{N-1} < r < a_N = b; \end{cases} \quad (4)$$

where  $u_j = \sqrt{n_j^2 \omega_L^2 / c^2 - \beta^2}$ ,  $n_j$  is the optical refractive factor of the  $j$ th layer with the radius from  $a_{j-1}$  to  $a_j$ ,  $w = \sqrt{\beta^2 - n_{cl}^2 \omega_L^2 / c^2}$ ,  $n_{cl}$  is the optical cladding refractive factor,  $J_0$  and  $N_0$  are respec-

tively Bessel functions of the first and second types (an order is "0"),  $A_{jk}$  are values, which are determined based on the optical boundary conditions.

There are many acoustic modes in the optical fiber.

The overlap factor of the acousto-optic interaction ( $I_{AOm}$ ) is determined as the ratio of the light effective area ( $A_L$ ) to the acoustic-optical interaction area ( $A_{Am}$ ) of the acoustic mode of the  $m$ th order by next formulas:

$$I_{AOm} = A_L / A_{Am}, \quad A_{Am} = \left( \frac{\{L^2(r)\}}{\{L^2(r) \cdot \xi_m(r)\}} \right)^2 \{ \xi_m^2(r) \},$$

$$A_L = \frac{\{L^2(r)\}^2}{\{L^4(r)\}}, \quad (5)$$

where is an, and  $\xi_m(r)$  is the amplitude distribution over the cross section of the fiber of the acoustic mode of the  $m$ -th order in the case of axial symmetry [7, 8]. All values are averaged over the fiber cross-section [9, 11].

The strength of the acoustic-optical interplay is determined by the spatial distribution of the acousto-optic interaction area over the fiber's cross-section. This factor is important for describing the MBB characteristics of the given fiber structure. Only one optical mode is propagated in single-mode optical fibers.

When describing the MBB phenomenon, it is important to consider the spatial interaction of the single optical mode with multiple lower-order acoustical modes [6-11].

The acoustic modes  $\xi_m(r)$  behavior ( $m$ th is the acoustic mode order) in the case of axial symmetry of the fiber structure is defined from the solution of wave equations (similar to (3), but for acoustic waves):

$$\frac{\partial^2 \xi_m(r)}{\partial r^2} + \frac{\partial \xi_m(r)}{r \partial r} + \left( \frac{\omega_{Am}^2}{v_A^2(r)} - k_A^2 \right) \xi_m(r) = 0. \quad (6)$$

where  $\omega_A \approx k_A \sqrt{v_A^2 - i\omega_A \Gamma}$  is the acoustic cyclic frequency,

$k_A \approx \frac{\omega_A}{v_A} + \frac{i\Gamma}{2v_A k_A^2}$ ,  $\Gamma$  is damping factor [7], and  $v_A$  is the hyper-

acoustic wave velocity. If certain characteristics differ for various modes, the index ( $m$ ) is added in their designations when solving equation (6).

The longitudinal velocity ( $v_{Azj}$ ) and the radial (transversal) velocity ( $v_{Arj}$ ) of the hyper-acoustic wave [6-11], which can be differ in each layer with various acoustic properties in the fiber structure, are determined by the next formula ("z" is the longitudinal axis of the propagating signal):

$$v_{Az}, v_{Ar} = \begin{cases} v_{Az1}, v_{Ar1} & , \text{if } r \leq a_1; \\ v_{Azj}, v_{Arj} & , \text{if } a_{j-1} < r \leq a_j; \\ v_{AzN}, v_{ArN} & , \text{if } a_{N-1} < r \leq b; \end{cases} \quad (7)$$

The  $v_{Azi}$  and  $v_{Ari}$  related the coefficients of Lamé in the  $j$ th layer [12].

The acoustic boundary conditions link these components at the boundaries of each pair of layers [8, 9, 12]. The acoustical factor ( $n_{Aj}$ ) at the  $j$ th and  $(j+1)$ th fiber layers is determined as ratio  $v_{Aj} / v_{Aj+1}$ .

If the velocity of the acoustic wave in the fiber cladding is higher than in the fiber core ( $v_{Azl} < v_A < v_{Azj}$ ), then acoustic waves are concentrated predominantly in the fiber core in this case [7-12].

The displacement vector components ( $U_z$  and  $U_r$ ) in the case  $v_{Az1} < v_A < v_{Azj} \dots$  (and respectively  $v_{Ar1} < v_A < v_{Arj} \dots$ ) are found by the following system of expressions:

$$U_z(r) = \begin{cases} A_{11}J_0(h_1r) + B_{11}J_0(k_1r), & \text{if } r \leq a_1, \\ A_{21}I_0(\tilde{h}_2r) + A_{22}K_0(\tilde{h}_2r) + B_{21}J_0(k_2r) + B_{22}N_0(k_2r), & \text{if } a_1 < r \leq a_2, \\ A_{j1}I_0(\tilde{h}_jr) + A_{j2}K_0(\tilde{h}_jr) + B_{j1}J_0(k_jr) + B_{j2}N_0(k_jr), & \text{if } a_{j-1} < r \leq a_j, \\ A_{N1}I_0(\tilde{h}_Nr) + A_{N2}K_0(\tilde{h}_Nr) + B_{N1}J_0(k_Nr) + B_{N2}N_0(k_Nr), & \text{if } a_{N-1} < r \leq a_N, \end{cases} \quad (8)$$

$$U_r(r) = \begin{cases} A_{11}h_1J_0'(h_1r) + B_{11}k_1J_0'(k_1r), & \text{if } r \leq a_1, \\ A_{21}\tilde{h}_2I_0'(\tilde{h}_2r) + A_{22}\tilde{h}_2K_0'(\tilde{h}_2r) + B_{21}k_2J_0'(k_2r) + B_{22}k_2N_0'(k_2r), & \text{if } a_1 < r \leq a_2, \\ A_{j1}\tilde{h}_jI_0'(\tilde{h}_jr) + A_{j2}\tilde{h}_jK_0'(\tilde{h}_jr) + B_{j1}k_jJ_0'(k_jr) + B_{j2}k_jN_0'(k_jr), & \text{if } a_{j-1} < r \leq a_j, \\ A_{N1}\tilde{h}_N I_0'(\tilde{h}_Nr) + A_{N2}\tilde{h}_N K_0'(\tilde{h}_Nr) + B_{N1}k_N J_0'(k_Nr) + B_{N2}k_N N_0'(k_Nr), & \text{if } a_{N-1} < r \leq a_N, \end{cases} \quad (9)$$

where  $I_0$  and  $K_0$  are respectively modified Bessel functions of the first and second types (an order is "0"),  $h_j = \sqrt{\omega_A^2 / v_{zj}^2 - k_A^2}$ ,  $k_j = \sqrt{\omega_A^2 / v_{rj}^2 - k_A^2}$ ,  $\tilde{h}_j = ih_j$ ,  $\tilde{h}_j = \sqrt{k_A^2 - \omega_A^2 / v_{zj}^2}$ ,  $U_r(r) = \partial U_z(r) / \partial(r)$  [5, 8, 13], and  $J_0'(hr) = \partial J_0(hr) / \partial(hr)$ ,  $K_0'(hr) = \partial K_0(hr) / \partial(hr)$ ,  $I_0'(hr) = \partial I_0(hr) / \partial(hr)$ ,  $N_0'(kr) = \partial N_0(kr) / \partial(kr)$  are the first derivatives of the corresponding Bessel functions, "i" ( $i = \sqrt{-1}$ ) is "imaginary unit".

The  $A_{jk}$  and  $B_{jk}$  coefficients are determined from ratios of the acoustic indicators  $k_A$  and  $k_j$ , and the acoustic boundary conditions of neighboring layers [8, 9].

If acoustic velocities in layers are higher ( $v_{Azj} > v_A$ ), it is necessary to perform the following replacement in (8) and (9):

$$J_0(h_jr) \rightarrow I_0(\tilde{h}_jr), \quad N_0(h_jr) \rightarrow K_0(\tilde{h}_jr), \quad h_j \rightarrow \tilde{h}_j. \quad (10)$$

If the velocity of the acoustic wave in the core is higher than in the cladding ( $v_{Azl} > v_A > v_{Azj}$ ), then acoustic waves penetrate from the fiber core into the fiber cladding [6-8]. The arguments ( $\tilde{h}_j$ ) of the modified Bessel functions for the corresponding layers in this case ( $v_A > v_{Azj}$ ) become "imaginary". This corresponds to the transition in some relevant lines of the system of equations (8) and (9) to ordinary Bessel functions of the real argument ( $h_j$ ).

It is necessary in this case to perform the reverse replacement in (8) and (9):

$$\tilde{h}_j \rightarrow h_j, \quad I_0(\tilde{h}_jr) \rightarrow J_0(h_jr), \quad K_0(\tilde{h}_jr) \rightarrow N_0(h_jr). \quad (11)$$

The factors ( $g_{Am}$ ) of the acoustical-optical scattering in the optical fiber for each acoustic modes (which order is "m") are

calculated using the next formula:

$$g_{Am} = p_{12} \omega_L \beta_m \int_0^b L^2(r) U_z(r) r k_{Am} dr \quad \text{or} \\ = p_{12} \omega_L \beta_m \int_0^b \rho_m(r, z) r \xi_m(r) L^2(r) dr, \quad (12)$$

where  $p_{12} \approx 0.27$ ,  $\beta_m$  – is the acoustical mode (which order is "m") coefficient of the phase;  $\rho_m(r, z)$  is the longitudinal medium density function along optical wave-guide of the acoustical mode (which order is "m") [6-8].

Every acoustical mode parameters are calculated by the next expressions:

$$A_{Am}(\omega) = \frac{g_{Am}^2}{4\pi} \frac{\Gamma_m}{(\omega - \omega_L + \omega_m)^2 + 0.25 \cdot \Gamma_m^2} \quad \text{or} \\ = \frac{I_{AOm}}{4} \frac{\Gamma_m^2}{(f - f_L - f_m)^2 + 0.25 \cdot \Gamma_m^2}. \quad (13)$$

The concluding MBB spectrum characteristic is achieved by merging the frequency dependencies from each mode. It is assumed that the contribution from each acoustic modes are independent [6-12].

Combining the tested sections of various types of single-mode fibers into a common light wave-guide significantly reduces the time to remove frequency and other characteristics of the MBB. BOTDR reflectograms for the entire light wave-guide are determined simultaneously, and then the MBB parameters (including the MBB frequency characteristics) for each section are analyzed.

The differences between the OF-G.654 graphs of different types are clearly visible (Fig. 1-6, Table 1).

The values of BFS under different temperature conditions were calculated for all tested types of G.654 fibers, and their MBB parameters were determined (Table 1), based on experimental BOTDR reflectograms.

Analyzing the MBB frequency characteristics for all studied types of G.654 fibers, it can be noted that in all cases there is a single pronounced maximum, which was also observed in the various types of G.652 and G.657 fibers.

For example, the fibers G.653 (a cut-off wavelength is 1.31 microns), G.655 (a cut-off wavelength is 1.48 microns) and ErDF have from one to three additional (side) "peaks" of different levels [4-6].

The differences in the MBB frequency characteristics and the BFS values (Table 1) can be used to automate the processing of BOTDR reflectograms and the classification of varieties of fibers.

Incorporating of fiber segments of various types in the light wave-guides when using the BOTDR allows them to be used as a "label" ("marker"), including in passive optical networks (PONs) to identify optical channels after optical splitters.

## References

- [1] F. L. Barkov, Y. A. Konstantinov, A. I. Krivosheev, "A novel method of spectra processing for Brillouin optical time domain reflectometry," *Fibers*, 2020. Vol. 8, No. 9, pp. 1-11. DOI: 10.3390/FIB8090060

[2] A.I. Krivosheev, F.L. Barkov, Y.A. Konstantinov, et al., "State-of-the-Art Methods for Determining the Frequency Shift of Brillouin Scattering in Fiber-Optic Metrology and Sensing," *Instrum Exp Tech*, 2022. Vol. 65, pp. 687-710. DOI: 10.1134/S0020441222050268

[3] I. V. Bogachkov, "Research of the features of Mandelstam – Brillouin backscattering in optical fibers of various types," *T-Comm*, 2019. Vol. 13. No. 1, pp. 60-65. DOI: 10.24411/2072-8735-2018-10216

[4] I. V. Bogachkov, N. I. Gorlov, "Experimental investigations into characteristics of Mandelstam–Brillouin scattering in single-mode optical fiber of various types," *Instruments and Experimental Techniques*, 2023. Vol. 66, No. 5, pp. 775-781. DOI: 10.1134/S0020441223050068

[5] I. V. Bogachkov, N. I. Gorlov, "Research of the optical fibers structure influence on the acousto-optic interaction characteristics and the Brillouin scattering spectrum profile," *Journal of Physics: Conference Series*, 2022. Vol. 2182(1), 012088, pp. 1-9. DOI: 10.1088/1742-6596/2182/1/012088

[6] I. V. Bogachkov, N. I. Gorlov, "Research of the influence of optical fibers structure on the spectral characteristics of Mandelstam – Brillouin scattering," *Journal of Physics: Conference Series*, 2021. Vol. 1791, pp. 1-8. DOI: 10.1088/1742-6596/1791/1/012039

[7] A. B. Ruffin, M.-J. Li, X. Chen, A. Kobayakov, F. Annunziata, "Brillouin gain analysis for fibers with different refractive indices," *Opt. Lett.* 2005. Vol. 30, pp. 3123-3125.

[8] Y. Koyamada, S. Sato, S. Nakamura, H. Sotobayashi, W. Chujo, "Simulating and designing Brillouin gain spectrum in single-mode fibers," *Lightwave Technol.* 2004. Vol. 22, pp. 631-639.

[9] P. D. Dragic, "Estimating the effect of Ge doping on the acoustic damping coefficient via a highly Ge-doped MCVD silica fiber," *J. Opt. Soc. Am. B*. 2009. V. 26, pp. 1614-1620.

[10] L. Tartara, C. Codemard, J. Maran, R. Cherif, M. Zghal, "Full Modal Analysis of the Brillouin Gain Spectrum of an Optical Fiber," *Optics Com.* 2009. Vol. 282, pp. 2431-2436.

[11] K. Park, Y. Jeong, "A quasi-mode interpretation of acoustic radiation modes for analyzing Brillouin gain of acoustically antiguiding optical fibers," *Optics Express*. 2014. Vol. 22. No. 7, pp. 2-13.

[12] P.-C. Law, Y.-Sh. Liu, A. Croteau, P.D. Dragic, "Acoustic coefficients of P2O5-doped silica fiber: acoustic velocity, acoustic attenuation, and thermo-acoustic coefficient," *Optical Materials Express*. 2011. Vol. 1. No. 4, pp. 686-699.

[13] I. V. Bogachkov, N. I. Gorlov, "The Mandelstam – Brillouin backscatter spectrum profile evaluation in optical fibers of various types," *XV International Scientific and Technical Conference "Actual Problems of Electronic Instrument Engineering" – Proceedings*. Novosibirsk, 2021, pp. 422-427. DOI 10.1109/APEIE52976.2021.9647468

[14] N. I. Gorlov, I. V. Bogachkov, "An Analysis of the Influence of the Physical Layers Structure of Optical Fibers on the Mandelstam – Brillouin Scattering Characteristics," *Systems of Signal Synchronization, Generating and Processing in Telecommunications (SINKHROINFO-2020) – Proceedings*, Kaliningrad, 2020, pp. 1–4. DOI: 10.1109/SYNCHROINFO49631.2020.9166063

[15] I.V. Bogachkov, "A detection of strained sections in optical fibers on basis of the brillouin relectometry method," *T-Comm*. 2016. Vol. 10. No.12, pp. 85-91. EDN: XKNRVF

## ВЫЯВЛЕНИЕ РАЗНОВИДНОСТЕЙ ОДНОМОДОВЫХ ОПТИЧЕСКИХ ВОЛОКОН СО СМЕЩЕННОЙ ДЛИНОЙ ВОЛНЫ ОТСЕЧКИ НА ОСНОВЕ АНАЛИЗА ХАРАКТЕРИСТИК РАССЕЯНИЯ МАНДЕЛЬШТАМА – БРИЛЛЮЭНА

**Богачков Игорь Викторович**, Омский государственный технический университет (ОмГТУ), Омск, Россия, [bogachkov@mail.ru](mailto:bogachkov@mail.ru)

### Аннотация

В современном быстро изменяющемся мире существенно расширился состав производителей различных оптических материалов ("заготовок", "преформ"), которые являются основой при производстве оптических кабелей (ОК) и волокон (ОВ) на территории Российской Федерации в настоящее время. К важным задачам относится классификация разновидностей ОВ в ОК и определение их физических параметров. На основании найденных параметров рассеяния Манделштама - Бриллюэна (РМБ) можно выявить участки волоконных световодов, которые имеют отличия в продольных растяжениях. Это является основой метода бриллюэновской рефлектометрии, который используется для ранней диагностики потенциально ненадёжных участков в волоконных световодах. При этом особо важной проблемой является выявление конкретных видов волокон различных изготовителей, которые при этом имеют одинаковый тип и имеют общую область назначения. В данной статье были проанализированы данные экспериментальных исследований частотных (спектральных) характеристик РМБ в световодах, содержащих различные участки из одномодовых ОВ разных типов при разных условиях функционирования (различных температурных и продольных растягивающих воздействиях) с помощью бриллюэновского рефлектометра с зондированием во временной области (BOTDR). ОВ различных типов и изготовителей, для которых были проведены экспериментальные исследования и построены бриллюэновские рефлектограммы, которые позволили определить необходимые характеристики физического состояния ОВ, были предоставлены ЗАО "Москабель - Фуджикура" (г. Москва) и АО "Оптиковолокonné Системы" (г. Саранск). Особый интерес представляет ОВ рекомендации G.654, которое отличается от обычных ОВ (рекомендации G.652 и т. п. для одномодовых ОВ) смещением длиной волны отсечки. Одновременное исследование характеристик РМБ участков ОВ разных типов, объединённых в единый световод, позволяет значительно ускорить выявление частотных характеристик РМБ, а далее и распределения натяжения, затухания и т.д. по всей длине световода. Также необходимо определить частотные характеристики РМБ для каждой отличающейся секции световода. Представлены итоговые результаты обработки результатов измерений (в том числе при температурных изменениях). На их основании возможно выявить конкретный тип одномодового ОВ, а также автоматизировать обработку данных и определение необходимых характеристик РМБ и физического состояния ОВ.

**Ключевые слова:** одномодовое оптическое волокно, рассеяние Манделштама – Бриллюэна, бриллюэновская рефлектограмма, профиль бриллюэновского спектра, оптическое волокно рекомендации G.654, обнаружение оптического канала утечки информации, информационная безопасность волоконно-оптической системы связи

## Литература

1. *Barkov F.L., Konstantinov Y.A., Krivosheev A.I.* A novel method of spectra processing for Brillouin optical time domain reflectometry // *Fibers*, 2020. Vol. 8, No. 9, pp. 1-11. DOI: 10.3390/FIB8090060
2. *Krivosheev A.I., Barkov F.L., Konstantinov Y.A.* et al. State-of-the-Art Methods for Determining the Frequency Shift of Brillouin Scattering in Fiber-Optic Metrology and Sensing // *Instrum Exp Tech*, 2022. Vol. 65, pp. 687-710. DOI: 10.1134/S0020441222050268
3. *Bogachkov I.V.* Research of the features of Mandelstam – Brillouin backscattering in optical fibers of various types // *T-Comm: Телекоммуникации и транспорт*, 2019. Т. 13. № 1. С. 60-65. DOI: 10.24411/2072-8735-2018-10216
4. *Богачков И.В., Горлов Н.И.* Экспериментальные исследования характеристик рассеяния Мандельштама-Бриллюэна в одномодовых оптических волокнах различных видов // *Приборы и техника эксперимента*, 2023. № 5. С. 70-77. DOI: 10.31857/S0032816223050063
5. *Богачков И.В., Майстренко В.А., Горлов Н.И.* Исследование влияния структуры оптических волокон на характеристики акустооптического взаимодействия // *Динамика систем, механизмов и машин*, 2021. Т. 9, № 3. С. 86-94.
6. *Богачков И.В., Горлов Н.И.* Исследование влияния структуры оптических волокон на спектральные характеристики рассеяния Мандельштама – Бриллюэна // *Динамика систем, механизмов и машин*, 2020. Т. 8, № 4. С. 98-105.
7. *Ruffin A.B., Li M.-J., Chen X., Kobayakov A., Annunziata F.* Brillouin gain analysis for fibers with different refractive indices // *Opt. Lett.* 2005. Vol. 30., pp. 3123-3125.
8. *Koyamada Y., Sato S., Nakamura S., Sotobayashi H., Chujo W.* Simulating and designing Brillouin gain spectrum in single-mode fibers // *Lightwave Technol.* 2004. Vol. 22, pp. 631-639.
9. *Dragic P.D.* Estimating the effect of Ge doping on the acoustic damping coefficient via a highly Ge-doped MCVD silica fiber // *J. Opt. Soc. Am. B.* 2009. Vol. 26, pp. 1614-1620.
10. *Tartara L., Codemard C., Maran J., Cherif R., Zghal M.* Full Modal Analysis of the Brillouin Gain Spectrum of an Optical Fiber // *Optics Com.* 2009. Vol. 282, pp. 2431-2436.
11. *Park K., Jeong Y.* A quasi-mode interpretation of acoustic radiation modes for analyzing Brillouin gain of acoustically antiguiding optical fibers // *Optics Express*. 2014. Vol. 22, № 7, pp. 2-13.
12. *Law P.-C., Liu Y.-Sh., Croteau A., Dragic P.D.* Acoustic coefficients of P2O5-doped silica fiber: acoustic velocity, acoustic attenuation, and thermo-acoustic coefficient // *Optical Materials Express*. 2011. Vol. 1, № 4, pp. 686-699.
13. *Bogachkov I.V., Gorlov N.I.* The Mandelstam – Brillouin backscatter spectrum profile evaluation in optical fibers of various types // *XV International Scientific and Technical Conference "Actual Problems Of Electronic Instrument Engineering"* Proceedings. Novosibirsk, 2021, pp. 422-427. DOI 10.1109/APEIE52976.2021.9647468
14. *Богачков И.В., Горлов Н.И.* Анализ влияния структуры физических слоёв оптических волокон на характеристики рассеяния Мандельштама – Бриллюэна // *Системы синхронизации, формирования и обработки сигналов*, 2020. №3. С. 64-69.
15. *Богачков И.В.* Обнаружение натяжённых участков в оптических волокнах на основе метода бриллюэновской рефлектометрии // *T-Comm: Телекоммуникации и транспорт*. 2016. Том 10. №12. С. 85-91. EDN: XKNRVF

## Информация об авторе:

**Богачков Игорь Викторович**, доктор технических наук, доцент; профессор кафедры "Средства связи и информационная безопасность", Омский государственный технический университет (ОмГТУ), Омск, Россия, Senior Member IEEE, ORCID ID 0000-0002-7019-1784